

Quantitative measurement of the surface silicon interstitial boundary condition and silicon interstitial injection into silicon during oxidation

M. S. Carroll* and J. C. Sturm

Department of Electrical Engineering, Princeton University, Princeton, New Jersey 08544

T. Büyüklımanlı

Evans East, 104 Windsor Center, East Windsor, New Jersey 08520

(Received 11 October 2000; published 7 August 2001)

During the oxidation of silicon, interstitials are generated at the oxidizing surface and diffuse into the silicon. Boron diffusion was used to map the local interstitial supersaturation, the ratio of interstitial concentration to the equilibrium concentration of interstitials versus the distance above buried $\text{Si}_{0.795}\text{Ge}_{0.2}\text{C}_{0.005}$ layers during oxidation. The average interstitial supersaturation at the silicon surface, extrapolated from the depth profiles was ~ 25 and ~ 13 for 750°C and 850°C , respectively. Using the measured interstitial concentration at the surface, the silicon interstitial injection into the silicon is calculated for oxidation at 750°C and 850°C . Finally, it is found that the surface boundary condition remains relatively fixed for an interstitial injection rate ranging over four orders of magnitude.

DOI: 10.1103/PhysRevB.64.085316

PACS number(s): 73.40.Lq, 61.72.Ss

INTRODUCTION

As silicon devices become increasingly smaller their electrical characteristics become more sensitive to small amounts of dopant diffusion during the device processing. Due to the increasing cost of trial and error approaches to determine the optimal processing parameters, industry must rely more on numerical simulations of device processing to find the optimal parameters. It is well established that the diffusivity of dopants that diffuse via an interstitial(cy) mechanism are enhanced during oxidation of the silicon surface. However, key parameters that determine dopant diffusion such as the silicon self-interstitial(cy) equilibrium concentrations, self-interstitial(cy) diffusivities and the point defect boundary conditions at the surface are due to the difficulties in measuring these properties directly at the temperatures of interest, while indirect measurements of these quantities do not agree well with one another.¹ Therefore, a complete understanding of oxidation enhanced diffusion (OED) is important both for controlling and predicting how device processing will effect device dopant profiles,² and for fundamental studies of point defects in silicon.³ For brevity, a silicon self-interstitial will be described as an “interstitial” in the rest of this paper.

Recent reports indicate that the introduction of substitutional carbon into silicon can suppress the local interstitial concentration and effectively sink the interstitials generated by oxidation.^{4,5} In this paper, we describe the use of this property of substitutional carbon in $\text{Si}_{0.795}\text{Ge}_{0.2}\text{C}_{0.005}$ layers to experimentally determine the profile of interstitial atoms during oxidation of silicon, from which we determine the interstitial boundary condition at the surface during oxidation. Combining this with previous measurements of the interstitial transport product allows us to determine the number of interstitials injected into the silicon during oxidation at 750°C and 850°C .

EXPERIMENT

Test structures were grown to measure the local boron diffusivity throughout the surface region of samples containing zero (sample A), one (sample B), or two (sample C) buried $\text{Si}_{0.795}\text{Ge}_{0.2}\text{C}_{0.005}$ layers [Figs. 1(a), 1(b), and 1(c), respectively]. The test structures were epitaxial layers grown on silicon substrates using rapid thermal chemical vapor deposition (RTCVD) at temperatures between 600°C and 750°C using dichlorosilane, germane, and methylsilane as the silicon, germanium and carbon sources, respectively.⁶ Each test structure was grown on a *p*-type Czochralski (CZ) (100) silicon wafer and was grown on both the top and bottom surface of the silicon wafer because of the reactor geometry. The three different test structures were grown with four 25 nm thick boron marker layers that had peak concentrations of $(4-9) \times 10^{18} \text{ cm}^{-3}$ centered below the surface at 150, 450, 600, and 900 nm depths. Sample B was grown with one 20 nm thick $\text{Si}_{0.795}\text{Ge}_{0.2}\text{C}_{0.005}$ layer centered at 675 nm below the surface; sample C was grown with two 20 nm thick $\text{Si}_{0.795}\text{Ge}_{0.2}\text{C}_{0.005}$ layers centered at 300, and 675 nm below the surface. Depths of the boron layers differed from the nominal values, unintentionally, as much as 30% from sample to sample.

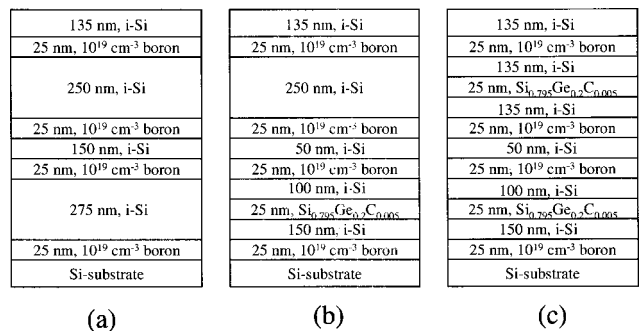


FIG. 1. Schematic diagram of the test structures A, B, and C [(a), (b), and (c), respectively] used in this experiment.

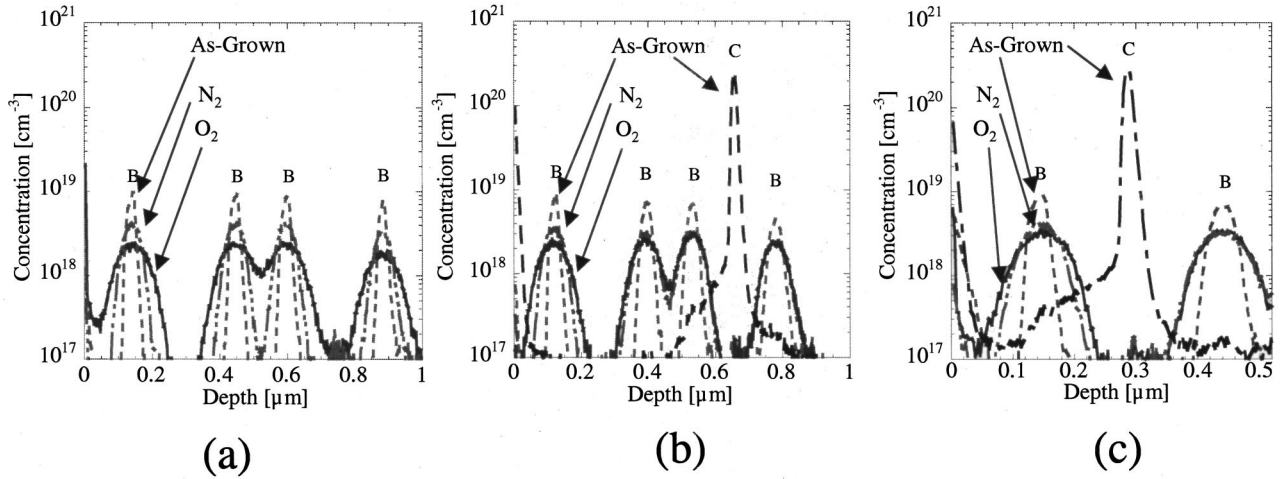


FIG. 2. Boron and carbon concentration profiles from SIMS of as-grown (dashed line, labeled *B* and *C* above the respective profiles) and boron concentrations for samples annealed for 30 min at 850 °C in either oxygen (solid line) or nitrogen (solid-dashed line) ambients for structures *A*, *B*, and *C* [(a), (b), and (c), respectively].

All test structures were cleaved and annealed in an oxygen or nitrogen ambient for various times between 30 and 960 min at 750 °C or 850 °C, and the resulting boron, carbon, germanium and oxygen profiles were obtained using secondary ion mass spectrometry (SIMS) done at Evans East in East Windsor, NJ. Samples were sputtered using 2 keV Cs⁺ ions, and depths were determined using standard profilometry of the sputtered craters leading to a 5% uncertainty in depths and a 20% uncertainty in boron concentration. The oxide growth rates measured by ellipsometry were 0.33 Å/min and 0.91 Å/min at 750 °C and 850 °C, respectively, in agreement with previous reports of thin silicon oxide films.⁷ No systematic difference was observed between the oxidation rate of silicon surfaces containing buried SiGeC layers and those without buried SiGeC layers.

Boron profiles of the pure silicon structure (sample *A*) after annealing at 850 °C for 30 min in oxygen or nitrogen ambient are noticeably broader than the as-grown case [Fig. 2(a)]. Moreover, the boron profiles in sample *A* after annealing in oxygen ambient are clearly broader, at all depths, than those after nitrogen anneal for the same time and temperature, indicative of the well documented oxygen enhanced diffusion effect.⁸ Boron profiles in the two samples containing Si_{0.795}Ge_{0.2}C_{0.005} layers before and after annealing in the identical conditions as in sample *A* [Figs. 2(b) and 2(c)] show different behavior above and below the buried Si_{0.795}Ge_{0.2}C_{0.005} layers. Boron profiles below the Si_{0.795}Ge_{0.2}C_{0.005} layers after 30 min of oxidation are identical to those after nitrogen anneal. As reported previously, the carbon layer prohibits interaction between the injected interstitials from the surface region and the boron below the carbon layer for this oxidation condition.⁴ This effect is due to the introduction of substitutional carbon and not due to the germanium.^{4,9} Boron profiles after oxidation above the Si_{0.795}Ge_{0.2}C_{0.005} layers are, however, broader than their respective counterparts annealed in nitrogen ambient. The differences in boron profile widths after oxidation versus nitrogen anneals, from marker to marker, are not however uniform. The profiles are clearly broader the nearer the boron

marker is to the surface [Fig. 2(b)]. The depth dependent diffusivity indicates a gradient in the interstitial concentration in the surface region. Boron concentration profiles after annealing in nitrogen or oxygen ambient were obtained for a number of different times and temperatures, 240, 480, and 960 min at 750 °C and 30, 60, and 120 min at 850 °C. The depth dependent diffusivity is most evident in the boron profiles after the longest anneal times, for example after 120 min oxidation at 850 °C (Fig. 3). Qualitatively, very similar profiles and depth dependent diffusivities were observed after annealing at 750 °C.

EXTRACTION OF DIFFUSIVITY ENHANCEMENT AND LINEARLY DECAYING INTERSTITIAL PROFILE

Average local boron diffusivities during annealing for each individual boron marker were extracted for each peak of each sample by using a standard process simulator, PROPHET,¹⁰ to numerically solve for the boron profiles after annealing, using the as-grown boron concentrations obtained by SIMS as the initial conditions. The process simulator solves the standard diffusion equation for dopants in silicon, which takes account of concentration and electric field dependent diffusivity. Because boron diffuses nearly entirely through an interstitial mechanism at temperatures near 800 °C,¹¹ the local boron diffusivity used to simulate the annealed boron profiles, depends on the local interstitial concentration as

$$\frac{D_B^{\text{meas}}}{D_B^*} \cong \frac{I}{I^*}, \quad (1)$$

where D_B^{meas}/D_B^* is the average boron diffusivity enhancement compared to the intrinsic diffusion (the asterisk indicates intrinsic value taken from literature) and I/I^* is the interstitial supersaturation. The boron diffusivity for the entire depth of the sample was adjusted for each marker layer by varying a single parameter to fit the annealed boron profile of each marker. The fitting parameter was the ratio of the

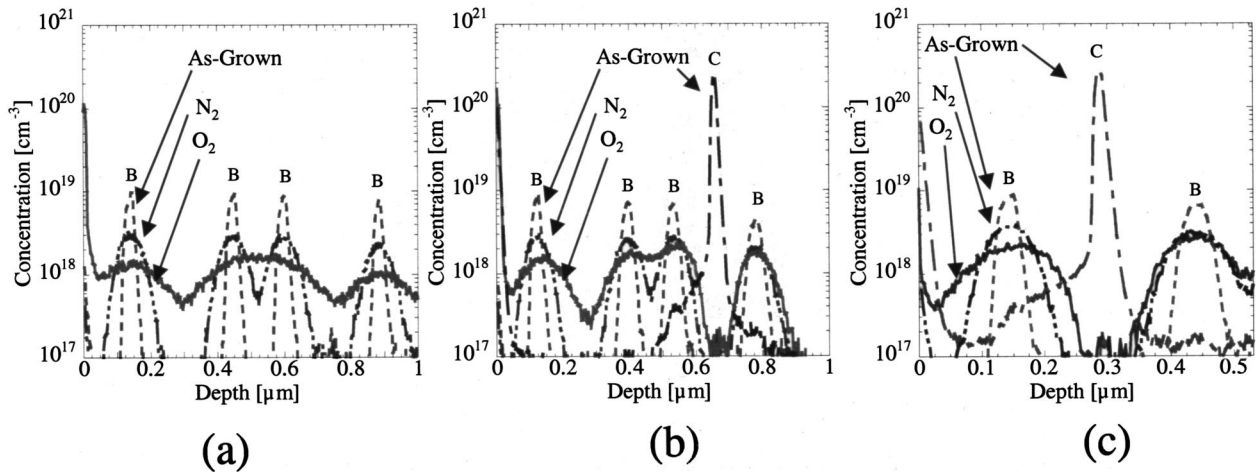


FIG. 3. Boron and carbon concentration profiles from SIMS of as-grown (dashed line, labeled *B* and *C* above the respective profiles) and boron concentrations for samples annealed for 120 min at 850 °C in either oxygen (solid line) or nitrogen (solid-dashed line) ambients for structures *A*, *B*, and *C* [(a), (b), and (c) respectively].

interstitial concentration to the intrinsic interstitial concentration, I/I^* . The interstitial enhancement for each marker during each oxidation for each time and temperature for all the samples obtained this way (see end of paragraph) are shown in Figs. 4 (750 °C) and 5 (850 °C). The boron diffusivity (i.e., the I/I^* ratio) measured during nitrogen anneals after all times examined for a sample *A* (pure silicon) were unity within the uncertainty of the measurement, and therefore agreed with those previously reported for the intrinsic boron diffusion in silicon (i.e., the boron diffusion observed during annealing in inert ambient).¹² Note that all boron diffusivities plotted at the SiGeC layer depths, shown in Figs. 4 and 5 as approximately zero, have been measured in a separate study^{13,14} as much smaller than the intrinsic boron diffusivity in silicon (even in cases of relatively high interstitial injection). The diffusivities shown for the sample *C* anneals of 60 or 120 min at 850 °C and 960 min at 750 °C were obtained by a second method explained in the following section.

The diffusivity enhancement for all the pure silicon samples (*A*) is found to be fairly uniform throughout the depth of the samples for both temperatures and all times, e.g., Fig. 4(a). This is consistent with previous reports of oxidation-enhanced-diffusion that demonstrate that the interstitial point defects, which enhance the boron diffusivity may

diffuse relatively long distances from the surface in a short time.¹⁵ The average diffusivity enhancement in silicon at 750 °C and 850 °C was found to be approximately 20.5 and 14.8 for the all silicon samples, consistent with previous reports of boron oxidation enhanced diffusion.⁹

Comparing the diffusivity enhancements from one oxidation time to another in a single sample shows that the enhancements remain relatively constant for all oxidation times. This indicates that the interstitial concentration is in a steady-state condition for these times. Furthermore, as shown in Figs. 4 and 5 in the samples with buried SiGeC layers, the I/I^* ratio during oxidation decays from the surface enhancement to approximately zero at the SiGeC layer and is well approximated by a linear profile versus depth.

The linear fits of the interstitial concentration can also be extrapolated to the surface of the silicon/oxide interface from the interstitial profiles in Figs. 4 and 5, and the average values (over each oxidation time) for each sample are displayed versus the depth of the SiGeC layers in Fig. 6. For comparison the surface concentrations obtained for sample *A* (no SiGeC layer) are shown on the same figure at a depth of 485 μm, the average depth of the back surface from the top surface. The uncertainty of the extrapolated interstitial surface concentrations, resulting from the uncertainty in the best lin-

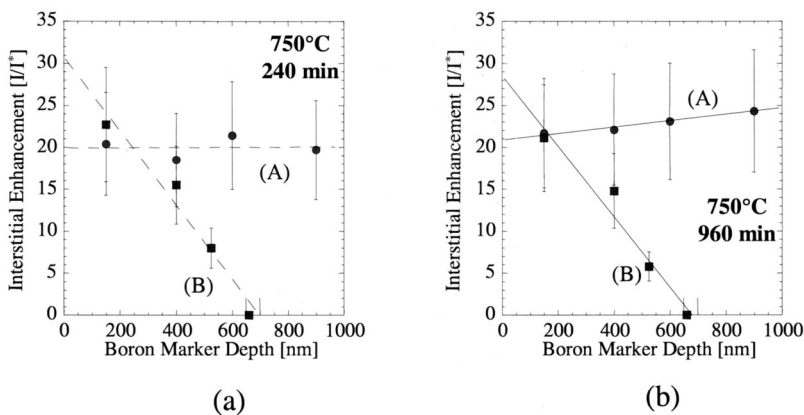


FIG. 4. Fitted boron diffusivity enhancements for all the samples and their marker depths are shown for oxidations at 750 °C for samples *A* and *B* after oxidation of (a) 240 min and (b) 960 min.

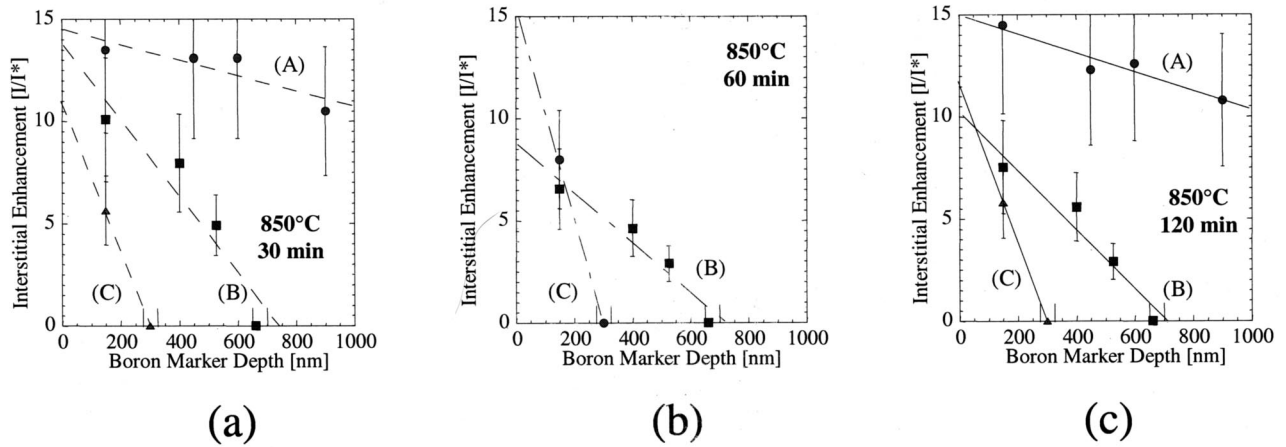


FIG. 5. Fitted boron diffusivity enhancements for all the samples and their marker depths are shown for oxidations at 850 °C for samples A, B, and C after oxidation of (a) 30 min, (b) 60 min (no values are available for sample A for this condition), and (c) 120 min.

ear fits, is indicated by the error bars in Fig. 6. The surface interstitial concentrations measured for each sample are within 20% of the average surface concentrations (averaged over all samples for each temperature), ~ 25 and ~ 12.7 for 750 °C and 850 °C, respectively. Effects from interstitials diffusing to the top region from the oxidizing back surface, that might affect the measured boron diffusivity enhancements, are neglected in cases B and C, because SiGeC layers were grown on both the top and bottom surfaces. Since the SiGeC layer on the back surface will react with injected interstitials from that surface first and the carbon content has been demonstrated to be enough to sink all injected interstitials, no additional interstitials are expected from the rear surface. This conclusion is supported by the lack of enhanced diffusion of the boron profiles below the SiGeC layer on the top surface. In case A (all-silicon sample) boron diffusivity enhancements have been previously found to be completely independent of the proximity of local interstitial sources and drains like a rear oxidizing surface as close as 20 μm ,^{16,17}

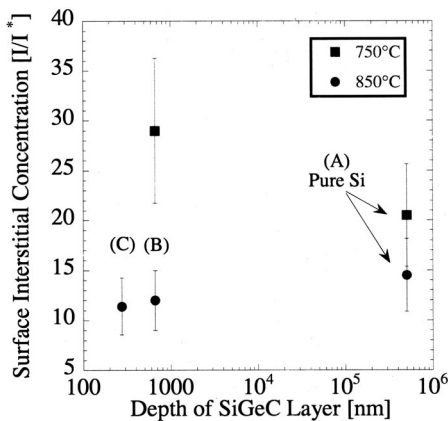


FIG. 6. Relative interstitial supersaturation at the surface of the silicon during oxidation estimated from the boron diffusivity enhancement profiles versus the SiGeC layer depth. For comparison, the depth of the rear surface is used to represent the pure silicon case located approximately 500 μm from the top surface.

which is consistent with this work's observation that the surface concentration is relatively independent of the depth of the interstitial sink, even when the nearby interstitial concentration is significantly altered by the presence of the interstitial sink.

BORON DIFFUSION IN A LINEAR DIFFUSIVITY GRADIENT

The above method for extraction of the boron diffusivity could be used as long as the boron peaks remained narrow and the ratio of I/I^* (or boron diffusivity enhancement) is approximately constant where the boron is diffusing. However, in sample C ($\text{Si}_{0.795}\text{Ge}_{0.2}\text{C}_{0.005}$ layer ~ 30 nm below the surface), the boron concentration profile after 120 min of oxidation at 850 °C and 960 min at 750 °C are very asymmetric [Fig. 3(c)] due to the diffusion in a steep interstitial gradient in the surface region. Near the surface the diffusion coefficient is substantially higher than near the SiGeC layer. It is no longer appropriate to extract a single diffusivity from the boron profiles in these cases. Therefore, for sample C it was necessary to simulate the boron diffusion in a diffusivity gradient to reproduce the asymmetric broadening and estimate the boron diffusivity enhancement. Boron profiles after annealing were simulated, using PROPHET, with a linearly decaying interstitial enhancement profile (i.e., boron diffusivity). The interstitial concentration was assumed pinned at zero at the SiGeC layer, and the interstitial enhancement at the surface ($n_{\text{surf}} = I_{\text{surf}}/I^*$) was used as a single adjustable parameter to fit simulated profiles with the data. Figure 7 shows the excellent fit of the modeling with the data, supporting the assumption of a linearly decaying interstitial enhancement profile. (For reference the carbon profiles before and after oxidation are also shown in Fig. 7 and also show that the carbon profile has not changed appreciably in the surface region.)

CALCULATION OF INTERSTITIAL INJECTION RATE

The interstitial concentration profiles may be used to deduce an interstitial flux in combination with the interstitial

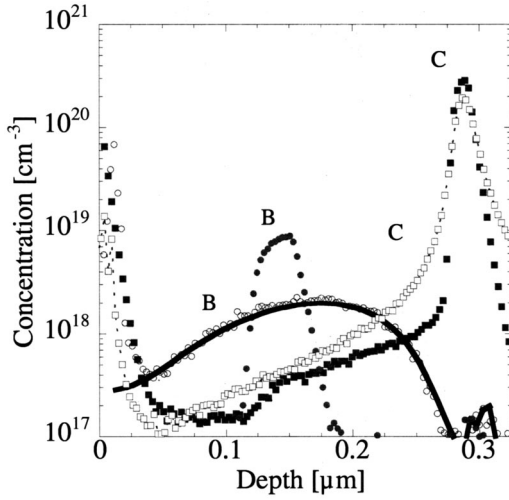


FIG. 7. (a) As-grown boron and carbon concentration profiles overlain on boron and carbon profiles after 120 min oxidation at 850 °C and simulated profile of the interstitial enhancement after oxidation for 120 min at 850 °C for sample C (SiGeC layer located 300 nm below the surface).

transport product $D_I^* I^*$ ($68 \text{ cm}^{-1} \text{ s}^{-1}$ and $1 \times 10^4 \text{ cm}^{-1} \text{ s}^{-1}$ for 750 °C and 850 °C, respectively) that has been measured reliably using metal tracer diffusion.¹ For samples B and C the silicon interstitial flux, J_I , injected into the silicon may be calculated by

$$J_I = -D_I^* \frac{dI}{dx} = n_{\text{surf}} \frac{D_I^* I^*}{\Delta x}, \quad (2)$$

where, Δx is the depth of the $\text{Si}_{0.795}\text{Ge}_{0.2}\text{C}_{0.005}$ layer, and n_{surf} is the experimentally obtained relative interstitial supersaturation at the surface (Fig. 6) and it is assumed that the interstitial concentration at the SiGeC layer is near zero.^{4,14} The total number of injected interstitials for samples B and C can be calculated by integrating the interstitial flux injected during oxidation [Eq. (2)] over the oxidation time (960 or 120 min at 750 °C or 850 °C, respectively), Fig. 8. In the case of pure silicon the interstitial diffusion length, assuming the self-interstitial diffusivities from Bracht's work, are of the order of the wafer dimension for the longest oxidation times, i.e., 792 μm or 685 μm for 960 or 120 min at 750 °C or 850 °C, respectively.¹ An order of magnitude estimate of the number of injected interstitials into sample A (pure silicon) can be made, therefore, by assuming that the interstitial concentration across the wafer depth equal to the surface concentration by these oxidation times.¹⁶ The total number of injected interstitials, therefore, is half the total increase of interstitials in the entire wafer, i.e., each surface contributes an equal number of interstitials,

$$Q_I = \frac{(n_{\text{surf}} - 1) \cdot I^* \cdot w}{2}, \quad (3)$$

where w is the width of the wafer ($\sim 485 \mu\text{m}$), Q_I is the total number of injected interstitials, and I^* is the literature value

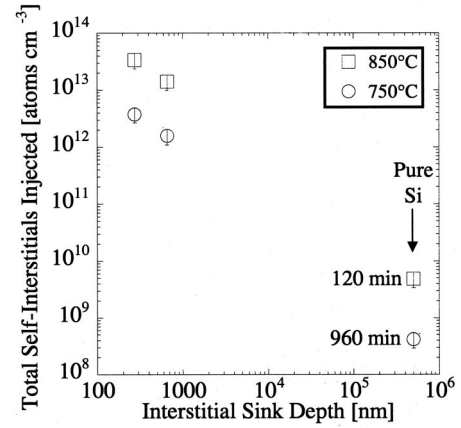


FIG. 8. The total interstitial atoms integrated over time injected into the silicon after 960 min at 750 °C or 120 min at 850 °C of oxidation versus the depth of the interstitial sink, i.e., the SiGeC layer or the bottom surface. The total interstitial areal densities were calculated using Eq. (2) or (3) and the measured surface supersaturation and SiGeC layer depths.

for the less well established silicon intrinsic concentration ($6.2 \times 10^8 \text{ cm}^{-3}$ or $1.54 \times 10^{10} \text{ cm}^{-3}$ for 750 °C and 850 °C, respectively¹).

Samples B and C (those with a buried SiGeC layer) show a significant increase in interstitial flux into the silicon bulk compared to sample A (pure silicon) in Fig. 8. The interstitial flux into the silicon bulk is governed by simple diffusion and is therefore determined entirely by the interstitial gradient. The calculated increase of interstitial injection due to the proximity of the SiGeC layer is, therefore, because the SiGeC layer acts as a local sink for injected interstitials reducing the interstitial concentration in the region directly below the surface, which in turn draws more interstitials from the surface into the bulk. When there is no SiGeC layer present the interstitial concentration rapidly increases and approaches the surface concentration, which reduces the interstitial gradient at the surface and therefore reduces the interstitial flux into the silicon from the surface (sample A, pure silicon).

DISCUSSION AND COMPARISON TO OTHER WORK

The observation that the surface supersaturation of interstitials remains unchanged (no more than 20% variation from the average) despite an increase of the total number of injected silicon interstitials qualitatively agrees with the proposed oxidation model by Dunham^{18–20} that predicts that the interstitial concentration at the silicon surface is pinned by a large reservoir of silicon interstitials that form and reside at the oxide/silicon interface above the silicon surface. This is the first report, of which the authors are aware, that shows the boundary condition remains constant, 850 °C, for interstitial injection rates ranging over four orders of magnitude. This demonstrates the stiffness of the surface boundary condition during oxidation and suggests that the surface concentration of interstitials in the silicon is determined by an interstitial reservoir at the silicon/oxide interface created by the oxidation.

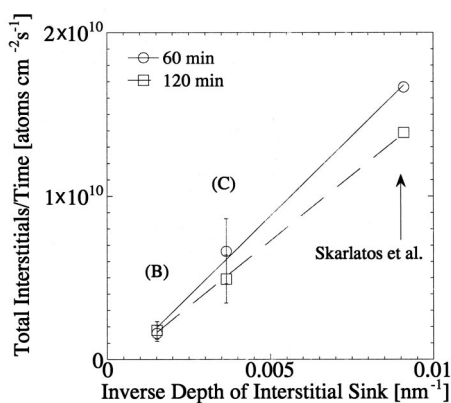


FIG. 9. The total number of injected silicon interstitials after oxidation measured using type II loop defects (Ref. 3) divided by the oxidation time (i.e., constant interstitial flux during oxidation) compared to the interstitial flux measured by the boron marker method (this work) is compared for their respective inverse depths. The linear fits for the two oxidation times show the flux is proportional to the inverse depth.

Recently, the integrated interstitial flux over time due to oxidation was also measured by monitoring the increase in size of type II loop defects located, 110 nm below the surface of an oxidized sample.³ The density of the loops is high enough to capture most of the injected interstitials, which make the loop defects an effective sink for injected interstitials. From Eq. (2), assuming that the interstitial profile decays linearly to zero at the interstitial sink (i.e., the loop defects), we may expect that the flux of interstitials into the sample with buried loop defects, during oxidation, is constant throughout the oxidation time and depends on the depth of the loop defects. To compare our work with theirs for different oxidation times and sink depth the total number of interstitials reported by the growth of loop defects is divided by the reported oxidation time (60 and 120 min) to obtain the constant flux during oxidation. The calculated flux for the loop defect experiment is compared to those calculated for the two samples B and C after 60 and 120 min of oxidation for their respective inverse depths. As can be seen in Fig. 9, the interstitial fluxes are proportional to the inverse depths of the interstitial sinks and therefore are well fit by a line for both times. The loop measurement of the total integrated interstitial injection agrees well with the boron marker measurements of interstitial injection during oxidation. Furthermore, the observation that the interstitial injection depends

inversely on the depth of the buried interstitial sink is also in agreement with the observed dependence of loop defect growth for loops located at varying depths from the surface after oxidation.²¹

Although both phosphorus and boron are believed to diffuse almost entirely by an interstitial(cy) mechanism^{11,22} the boron diffusion enhancements during oxidation are often slightly lower ($\sim 30\%$ at 850°C) than that of the phosphorus.^{20,23} A possible reason for this is boron cluster effects,⁵ which could temporarily trap mobile boron and reduce the effective diffusivity causing an underestimate of the true interstitial injection by the method presented in this work. However, the good agreement between the measurements in this work and that from the growth of loop defects, which is independent of boron clustering effects, indicates that there are no significant reductions in boron diffusivity leading to an appreciable underestimate of interstitial injection. No comparison was available for 750°C , which may be because the number of injected interstitials calculated from our data is far below the currently reported resolution of the loop defect method of $(2-3) \times 10^{13}$ atoms/cm². This demonstrates the sensitivity of our approach for measuring the total number of injected interstitials at very low injection rates.

CONCLUSION

In conclusion, the average boron diffusivity during oxidation above $\text{Si}_{0.795}\text{Ge}_{0.2}\text{C}_{0.005}$ layers has been used to map the profile of interstitials injected into silicon during oxidation, and also to quantify the total number of interstitials injected into the silicon substrate. The interstitial supersaturation concentration at the surface for 750°C and 850°C is determined and the average interstitial supersaturation concentration is found to depend weakly, if at all (850°C), on the rate of interstitial injection into the bulk silicon, despite increasing the total number of injected interstitials by four orders of magnitude. Finally, this method is an exceedingly sensitive measure of injected interstitial fluxes.

ACKNOWLEDGMENTS

The authors would like to thank H. Rücker and C. S. Rafferty for helpful discussion and providing computer script for simulation of carbon diffusion. This work was supported by ONR/DARPA (N66 001-97-8904) and ARO/MURI (DAA 655-98-1-0270).

*Electronic mail: malcolmc@ee.princeton.edu

¹H. Bracht, N. A. Stolwijk, and H. Mehrer, *Phys. Rev. B* **52**, 16 542 (1995).

²M. Yang, C.-L. Chang, M. Carroll, and J. C. Sturm, *IEEE Electron Device Lett.* **20**, 301 (1999).

³D. Skarlatos, M. Omri, A. Claverie, and D. Tsoukalas, *J. Electrochem. Soc.* **146**, 2276 (1999).

⁴M. Carroll, C.-L. Chang, J. C. Sturm, and T. Buyuklimanli, *Appl. Phys. Lett.* **73**, 3695 (1998).

⁵P. A. Stolk, H.-J. Gossmann, D. J. Eaglesham, D. C. Jacobson, C. S. Rafferty, G. H. Gilmer, M. Jaraiz, J. M. Poate, H. S. Luft-

mann, and T. E. Haynes, *J. Appl. Phys.* **81**, 6031 (1997).

⁶J. C. Sturm, P. V. Schwartz, E. J. Prinz, and H. Manoharan, *J. Vac. Sci. Technol. B* **9**, 2011 (1991).

⁷E. A. Irene, *J. Electrochem. Soc.* **125**, 1708 (1978).

⁸D. A. Antoniadis and I. Moskowitz, *J. Appl. Phys.* **53**, 6788 (1982).

⁹P. Kuo, J. L. Hoyt, J. F. Gibbons, J. E. Turner, and D. Lefforge, *Appl. Phys. Lett.* **67**, 706 (1995).

¹⁰M. R. Pinto, D. M. Boulin, C. S. Rafferty, R. K. Smith, W. M. Coughran, I. C. Kizilyalli, and M. J. Thoma, *Tech. Dig Int. Electron Devices Meet.* 923 (1992).

- ¹¹H.-J. Gossmann, T. E. Haynes, P. A. Stolk, D. C. Jacobson, G. H. Gilmer, J. M. Poate, H. S. Luftman, T. K. Mogi, and M. O. Thompson, *Appl. Phys. Lett.* **71**, 3862 (1997).
- ¹²R. B. Fair, *Processing Technologies* (Academic, New York, 1981), Vol. Supplement 2B.
- ¹³M. S. Carroll, L. D. Lanzerotti, and J. C. Sturm, in *Quantitative Measurement of Reduction of Boron Diffusion by Substitutional Carbon Incorporation* (Materials Research Society, San Francisco, 1998), p. 417.
- ¹⁴R. F. Scholz, P. Werner, U. Goesele, and T. Y. Tan, *Appl. Phys. Lett.* **74**, 392 (1999).
- ¹⁵H.-J. Gossmann, C. S. Rafferty, H. S. Luftmann, F. C. Unterwald, T. Boone, and J. M. Poate, *Appl. Phys. Lett.* **63**, 639 (1993).
- ¹⁶S. T. Ahn, J. D. Shott, and W. A. Tiller, Abstract No. 545 (Electrochemical Society, Pennington, NJ, 1986).
- ¹⁷P. M. Fahey, P. B. Griffin, and J. D. Plummer, *Rev. Mod. Phys.* **61**, 289 (1989).
- ¹⁸S. T. Dunham and J. D. Plummer, *J. Appl. Phys.* **59**, 2551 (1986).
- ¹⁹S. T. Dunham and J. D. Plummer, *J. Appl. Phys.* **59**, 2541 (1986).
- ²⁰S. T. Dunham and J. D. Plummer, *J. Appl. Phys.* **71**, 685 (1992).
- ²¹D. Tsoukalas, D. Skarlatos, and J. Stoemenos, *J. Appl. Phys.* **87**, 8380 (2000).
- ²²A. Ural, P. B. Griffin, and J. D. Plummer, *J. Appl. Phys.* **85**, 6440 (1999).
- ²³D. J. Roth and J. D. Plummer, *J. Electrochem. Soc.* **141**, 1074 (1994).